Oxidation of (Carboxyalkyl)thiopropionic Acid Derivatives by Hydroxyl Radicals. Mechanisms and Kinetics of Competitive Inter- and Intramolecular Formation of σ- and σ^*-type Sulfuranyl Radicals

Krzysztof Bobrowski,*,†,‡ Dariusz Pogocki,† and Christian Schöneich*,§

Institute of Nuclear Chemistry and Technology, Dorodna 16, 03-195 Warsaw, Poland; Radiation Laboratory, University of Notre Dame, Notre Dame, Indiana 46556; and Department of Pharmaceutical Chemistry, University of Kansas, Lawrence, Kansas 66047

Received: July 23, 1998; In Final Form: October 15, 1998

The substituent effects on kinetics and yields of specific intermediates and products for the one-electron oxidation by hydroxyl radicals of various (carboxylalkyl)thiopropionic acid derivatives, 3-(methylthio)propionic acid (3-MTPA), 3,3′-thiodipropionic acid (3,3′-TDPA), 3-(carboxymethylthio)propionic acid (3-CMTPA), and 2-(carboxymethylthio)succinic acid (2-CMTPA) have been investigated employing pulse radiolysis on the nanosecond to microsecond time scale, and γ-radiolysis. For each derivative, the initial step was a formation of a hydroxysulfuranyl radical proceeding with absolute rate constants of $k_{OH+3\text{-MTPA}} = 9.1 \times 10^9$ M^{-1} s^{-1} and $k_{OH+3,3'\text{-TDPA}} = 5.8 \times 10^9$ M^{-1} s^{-1}. The subsequent formation of one-electron-oxidized intermediates such as dimeric sulfur−sulfur (S∴S)-three-electron-bonded and monomeric sulfur−carboxylate oxygen (S−O)-bonded sulfide radical cations strongly depended on pH, thioether concentration, and the availability of α- or β-positioned carboxylate functions. A spectral resolution procedure permitted the quantification of all transients present in solution at any time after the pulse. Whereas both (S∴S)- and (S−O)-bonded intermediates were formed for 3-MTPA at neutral solution, electrostatic repulsion nearly prohibited the formation of dimeric (S∴S)-bonded intermediates between an overall negatively charged sulfide radical cation of 3,3′-TDPA and a second nonoxidized, overall twice negatively charged, molecule of 3,3′-TDPA. Neither sulfide radical cation complex $(S\therefore S)^+$ was observed for 3-CMTPA and 2-CMPTA rationalized by a fast decarboxylation of the α-positioned carboxylate group, yielding α-(alkylthio)alkyl radicals which were the only products optically observed on the pulse radiolysis time scale. For 3,3′-TDPA, the conversion of the initially formed hydroxysulfuranyl radicals into the (S−O)-bonded intermediates occurred unimolecularly with $k \cong 10^8$ s^{-1} whereas the formation of the (S∴S)-bonded intermediates proceeded bimolecularly with $k = (1.9-2.0) \times 10^8$ M^{-1} s^{-1}. These processes did not occur competitively, as the intercepts of plots of pseudo-first-order rate constants for the formation of the S∴S bonded intermediates as a function of thioether concentration were too small (2.7×10^7 s^{-1}) to contain the unimolecular rate constant for the formation of the (S−O)-bonded intermediate ($k = 10^8$ s^{-1}). Therefore, a mechanism was proposed according to which initially formed hydroxysulfuranyl radicals rapidly converted into the σ^*-type (S−O)-bonded intermediate. Subsequently, these either converted into (S∴S)-bonded radical cation complexes via a displacement of the carboxylate oxygen by a second nonoxidized sulfide function, or reversibly ring-opened to yield the monomeric sulfur-centered radical cation. The latter either associated with a nonoxidized sulfide or irreversibly cyclized to a σ-type (S−O)-bonded sulfuranyl radical.

Introduction

Thioethers are preferred targets of reactive oxygen species[1−6] including the highly reactive hydroxyl radical.[7−9] Therefore, considerable research effort has been undertaken to elucidate factors that control such oxidation reactions.[7] The participation of neighboring groups has been identified as one crucial mechanistic detail.[10] In general, neighboring groups act catalytically through transient bond formation between sulfur radical cationic intermediates and electron lone-pair carrying functional groups[7] such as oxygen, nitrogen, sulfur, phosphorus, and selenium. In many but not all cases these transient bonds have been characterized as three-electron bonds with their respective strength being dependent on the difference in electronegativity between the bond-forming atoms as well as on structural parameters.[7] Although existence, stability, physicochemical properties, and subsequent reactions of these intermediates have been well studied, considerably less information is available about their formation mechanisms. Studies of this kind are necessary not only for biochemical pathways, e.g., oxidative stress, but increasingly also for atmospheric oxidation processes where the involvement of hydroxyl radicals has been invoked.[11]

Initially, the reaction of a hydroxyl radical with a thioether sulfur yields a hydroxysulfuranyl radical[12] which subsequently decomposes via several routes for which the rate constants can vary by as much as 2 orders of magnitude depending on the nature of the thioether. For example, recently the formation of a relatively stable hydroxysulfuranyl radical of 2-(methylthio)-acetic acid methyl ester[13,14] has been reported which decomposes

† Institute of Nuclear Chemistry and Technology.
‡ University of Notre Dame.
§ University of Kansas.

10.1021/jp983136g CCC: $15.00
Published on Web 11/26/1998

CHART 1

$H_3C-S-CH_2-CH_2-COOH$
3-(Methylthio)propionic Acid
[3-MTPA] a

$HOOC-CH_2-CH_2-S-CH_2-CH_2-COOH$
3,3′-Thiodipropionic Acid
[3,3′-TDPA] b

$HOOC-CH_2-S-CH_2-CH_2-COOH$
3-(Carboxymethylthio)propionic Acid
[3-CMTPA] c

$HOOC-CH_2-\underset{\underset{COOH}{|}}{CH}-S-CH_2-COOH$
2-(Carboxymethylthio)succinic Acid
[2-CMTSA] d

ca. 20-fold slower than the corresponding hydroxysulfuranyl radical from dimethyl sulfide.[15] In contrast, hydroxysulfuranyl radicals are significantly less stable for the corresponding 2-(methylthio)acetic acid and 2,2′-thiodiethanoic acid where intramolecular proton transfer catalyzes sulfur radical cation formation followed by decarboxylation,[16] and for 2-(methylthio)-ethanol and 2,2′-dihydroxydiethyl sulfide where a rapid intramolecular hydrogen transfer from the adjacent hydroxyl groups leads to (alkylthio)ethoxy radicals.[15]

Decarboxylation is thermodynamically unfavorable for 3-(methylthio)propionate where instead the initially formed sulfur radical cation can stabilize through intramolecular sulfur−oxygen and intermolecular sulfur−sulfur bond formation.

The present paper provides a detailed kinetic and mechanistic evaluation of the processes leading to sulfur−nucleophile bond formation during the hydroxyl radical induced oxidation of 3-(methylthio)propionic acid and its derivatives (Chart 1). Important parameters are the number and location of the carboxylate groups with respect to the thioether function and the pH of the solution. The formation kinetics and relative yields of the different sulfur−nucleophile-bonded species vary depending on the structure of the sulfide. They are further complicated by the fact that different electronic configurations of the sulfur−oxygen intermediates can exist such as σ-, π-, and σ*-type radicals.[17] Structures of the sulfuranyl radicals have been the subject of several investigations. In the σ-type structure, the sulfur atom and its three nearest neighbors adopt a T shape with the unpaired electron localized in an orbital which is in the plane of those atoms and centered mainly on the sulfur atom. On the other hand, in the σ*-type structure, the configuration about the sulfur atom is pyramidal. The unpaired electron is located in an antibonding orbital associated with the bond between the sulfur atom and one of its ligands and could be subject to delocalization depending on suitably located energy levels in the MO diagram. The distinction between the both structures is fairly subtle since the transition from the σ-type structure to the σ*-type structure requires a change from a planar to a pyramidal configuration about the sulfur atom. Which of these electronic structures describes best certain chemical properties will depend on structural parameters and substitution patterns. The structure of radicals such as $CF_3SS^{\bullet}R_2$, $RC(O)SS^{\bullet}R_2$, $(CH_3)_3SiOS^{\bullet}R_2$, and $R_2S^{\bullet}X$ is described in terms of the σ*-type structure.[17d] The sulfuranyl radicals $(CF_3O)_3S^{\bullet}$, $(RO)_3S^{\bullet}$, and $(RO)_2S^{\bullet}F$ probably adopt a planar T-shaped structure and can be described in terms of the σ-type structure.[17e]

Based on theoretical calculations and parallel UV and ESR experiments,[17] it has been suggested that σ*- and σ-type sulfuranyl radicals absorb in the 390 nm region whereas π-type

CHART 2

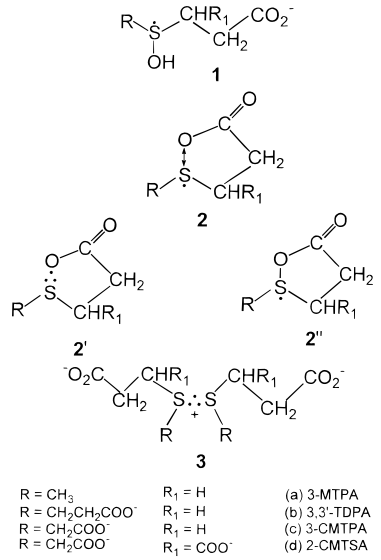

sulfuranyl radicals absorb in the 340 nm region. So far, pulse radiolytically[18] and laser flash photolytically[19] observed sulfur−oxygen-bonded intermediates have generally been assigned to the σ*-type radicals though based on spectroscopic analysis alone they cannot be distinguished from the σ-type radicals.[17] Our present results will provide kinetic evidence for the formation of both σ*- and σ-type sulfuranyl radicals (see Chart 2) parallel and/or after the decomposition of initially formed hydroxysulfuranyl radicals of (carboxyalkyl)thiopropionic acids.

Experimental Section

Materials. The sulfur-containing carboxylic acids, 3-(methylthio)propionic acid (3-MTPA) and 3,3′-thiodipropionic acid (3,3′-TDPA), were purchased from Lancaster (Windham, NH) and Sigma, respectively. They were of the purest commercially available grade and were used as received. 3-(Carboxymethylthio)propionic acid (3-CMTPA) and 2-(carboxymethylthio)-succinic acid (2-CMTSA) were obtained from Fluka and Aldrich, respectively, and were three times crystallized from water prior to the experiment. $HClO_4$ (redistilled) was from Aldrich, NaOH from Fisher, and *tert*-butyl alcohol from J. T. Baker. Water was purified by a Millipore-Milli-Q system.

Solutions. All solutions were made up freshly and bubbled for at least 30 min per 100 mL sample with N_2O or N_2. The respective pH's, if necessary, were adjusted with NaOH or $HClO_4$ and measured with an Orion glassy and calomel pH electrode coupled to an Orion pH-meter 811.

Pulse Radiolysis. All pulse radiolysis experiments were performed at the Radiation Laboratory by applying 10 ns pulses of high-energy electrons from the Notre Dame 7 MeV ARCO LP-7 linear accelerator. Absorbed doses were in the order of 4−6 Gy (1 Gy = 1J/kg). Signal averaging methods were used. Dosimetry was based on the N_2O-saturated thiocyanate dosimeter using a radiation chemical yield of $G = 6.13$ (G denotes the numbers of species formed or converted per 100 eV absorbed energy; $G = 1.0$ corresponds to 0.1036 μmol/J absorbed energy in aqueous solution; for practical purposes the G unit rather than the SI unit is used throughout this paper) and an extinction coefficient of 7580 M^{-1} cm^{-1} at 472 nm for $(SCN)_2^{\bullet-}$.[20] A description of the pulse radiolysis setup, data collection, and details of dosimetry has been reported elsewhere.[21,22] The data acquisition subsystem has been updated[23] and includes a Spex 270M double monochromator, a LeCroy 7200A transient

digitizer, and a PC-AT compatible computer. The software was written[23] within LabWindows of National Instruments. The experiments were carried out with the solution flowing continuously.

γ-Radiolysis. Steady-state γ-radiolysis experiments were carried out in the field of a 6000 Ci ^{60}Co-γ-source (Hahn-Meitner-Institut Berlin, Germany) using a dose rate of 16.7 Gy/min and in the field of a 16 600 Ci ^{60}Co-γ-source (Issledovatel, USSR) (Institute of Nuclear Chemistry and Technology, Warsaw, Poland) using a dose rate of 118 Gy/min measured by Fricke dosimetry.[24] Generally, the radiolytic conversion of sulfur-containing acids was less than 15% in order to avoid subsequent reactions of primary radicals with reaction products.

Analysis of Carbon Dioxide. The quantitative carbon dioxide analysis was achieved employing the gas chromatographic headspace technique (over the pH range 1.0−3.5) or high-performance ion chromatography (HPIC) at pH > 3.5. Details of both methods are described elsewhere.[25]

Results

Pulse Radiolysis. Pulse irradiation of water leads to the formation of the highly reactive species shown in reaction 1.[26]

$$H_2O \rightarrow e_{aq}^-, {}^\bullet OH, {}^\bullet H \quad (1)$$

In N_2O-saturated solutions ($[N_2O]_{sat} \approx 2.0 \times 10^{-2}$ M)[21] the hydrated electrons are converted into hydroxyl radicals according to reaction 2 ($k_2 = 9.1 \times 10^9$ M^{-1} s^{-1})[21] giving the total initial yield of hydroxyl radicals of $G^0({}^\bullet OH) = 6.1$, [26] available for further studies.

$$e_{aq}^- + N_2O \rightarrow N_2 + {}^\bullet OH + OH^- \quad (2)$$

At pH < 4 the diffusion-controlled reaction of e_{aq}^- with protons becomes important (reaction 3, $k_3 = 2.0 \times 10^{10}$ M^{-1} s^{-1}),[27] resulting in a pH-dependent reduced yield of hydroxyl radicals.

$$e_{aq}^- + H^+ \rightarrow {}^\bullet H \quad (3)$$

The reaction of ${}^\bullet OH$ radicals with thioethers generally proceeds to an extent of ca. 80% via addition to the thioether moiety, yielding hydroxysulfuranyl radicals (reaction 4)[8a]

$$ {}^\bullet OH + S\langle \rightarrow \rangle S^\bullet - OH \quad (4)$$

and to an extent of ca. 20%[8a] via hydrogen abstraction at the α-(alkylthio)carbon−hydrogen bond, yielding α-(alkylthio)alkyl radicals (reaction 5).

$$ {}^\bullet OH + -CH_2-S-CH_2- \rightarrow -{}^\bullet CH-S-CH_2- + H_2O \quad (5)$$

Absorption Spectra. *3-(Methylthio)propionic Acid (3-MTPA).* The reaction of ${}^\bullet OH$ radicals with 3-MTPA was investigated in both N_2O- and N_2-saturated solutions of 3-MTPA over the concentration range of 2×10^{-4}−10^{-2} M, and at various pH values. Depending on the pH and the concentration of the solute, pulse irradiation leads to different transient optical spectra. A broad absorption was observed in the 260−600 nm range with $\lambda_{max} = 430$ nm and a pronounced shoulder around 340−380 nm, 50 ns after pulse irradiation of an N_2O-saturated, pH 5.7, solution containing 10^{-2} M 3-MTPA (Figure 1A, curve a). After ca. 800 ns, the transient absorption spectrum was dominated by the 480 nm absorption (Figure 1A, curve b) which

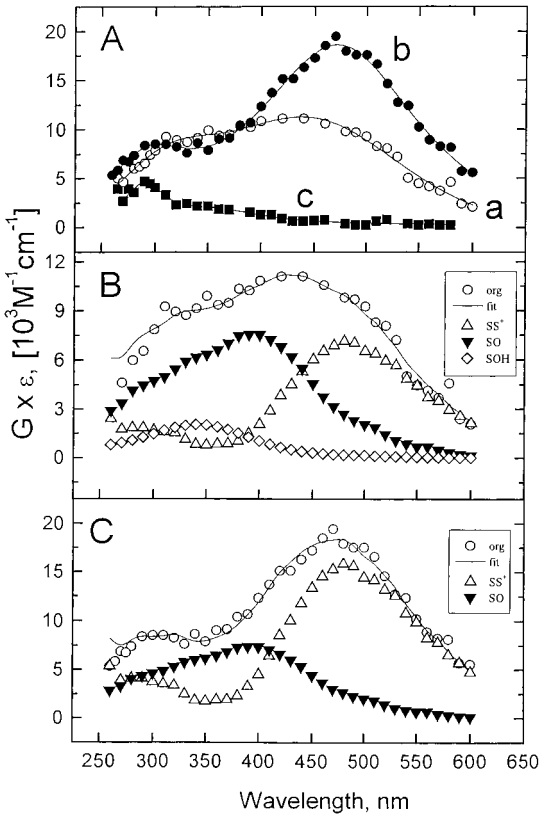

Figure 1. (A) Transient absorption spectra observed (a) 50 ns, (b) 800 ns, and (c) 30 μs after pulse irradiation of an N_2O-saturated aqueous solution containing 10^{-2} M 3-MTPA at pH 5.7. **(**B) Resolution of the spectral components in the transient absorption spectrum following the ${}^\bullet OH$-induced oxidation of 3-MTPA (10^{-2} M) at pH 5.7 taken 50 ns after the pulse. (C) Resolution of the spectral components in the transient absorption spectrum following the ${}^\bullet OH$-induced oxidation of 3-MTPA (10^{-2} M) at pH 5.7 taken 800 ns after the pulse.

then practically disappeared within 30 μs after the pulse, leaving a UV band with $\lambda_{max} = 285$ nm (Figure 1A, curve c). It may be anticipated (and is supported by the experimental findings and resolving procedure described below) that the spectra recorded represent the combined absorption bands of intramolecularly (${}^\bullet S \leftrightarrow O$)-bonded radicals **2a**[28] with $\lambda_{max} = 400$ nm, parts of the initially formed hydroxysulfuranyl radical **1a** with $\lambda_{max} = 340$ nm, and the intermolecularly sulfur−sulfur-bonded dimeric radical cation **3a** with $\lambda_{max} = 480$ nm (see the respective structures in Chart 2).

The composite spectra in Figure 1A (curves a and b) were resolved into component transients by a linear regression technique[29] of the form

$$G\epsilon(\lambda_j) = \sum \epsilon_i(\lambda_j) G_i \quad (I)$$

where $G\epsilon(\lambda_j)$ is the observed absorbance change of the composite spectrum depicted in radiation chemical yield units and $\epsilon_i(\lambda_j)$ is the molar absorption coefficient of the ith species at the jth wavelength of observation. The linear regression coefficients G_i correspond to the radiation chemical yield of the ith transient. Equation I takes on a form that is analogous to the linear regression analysis that was used to resolve the transient spectra in flash photolysis studies. Further details of this method have been described elsewhere.[30]

The individual contributions of the component spectra at every wavelength, $\{\epsilon_i(\lambda_j)\}$, of the transients **2a** and **3a** have been obtained from the spectra recorded over a wide wavelength

TABLE 1: Spectral Data of Intermolecular $(S\therefore S)^+$-Type Dimeric Radical Cations and Intramolecular ($^\bullet$S−O)-Type Radicals for 3-(Methylthio)propionic acid (3-MTPA) and 3,3′-Thiodipropionic acid (3,3′-TDPA) in Aqueous Solutions Obtained by the Pulse Radiolysis

	$(S\therefore S)^+$		($^\bullet$S−O)	
acid	λ_{max} (nm)	ϵ (M^{-1} cm^{-1})	λ_{max} (nm)	ϵ (M^{-1} cm^{-1})
3-MTPA	480	9200[a,b]	390	2500[d,e]
3,3′-TDPA	500	8250[a,c]	390	2900[d,f]

[a] Taking $G(S\therefore S)^+ = 2.4$ which is 80% of the available $^\bullet$OH radicals, total $G(^\bullet OH) = 3.0$, standard deviation of measurements ±10%. [b] [3-MTPA] = 10^{-2} M, pH = 1, N_2-saturated. [c] [3-TDPA] = 10^{-1} M, pH = 1, N_2-saturated. [d] Taking $G(^\bullet S{-}O) = 4.25$ which is 80% of the available $^\bullet$OH radicals, total $G(^\bullet OH) = 5.3$, standard deviation of measurements ±10%. [e] [3-MTPA] = 2×10^{-4} M, pH = 6.5, N_2O-saturated. [f] [3,3′-TDPA] = 2×10^{-4} M, pH = 6.0, N_2O-saturated.

range (260−600 nm) and under experimental conditions where one can expect an exclusive formation of either species **2a** or **3a**. For example, the spectrum of the intramolecularly sulfur−oxygen-bonded radical **2a** was obtained from pulse irradiations of an N_2O-saturated aqueous solution of 3-MTPA (2×10^{-4} M) at pH = 6.5 where **2a** forms according to reaction 6. The

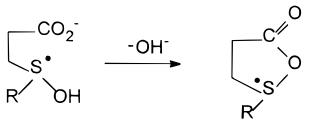

(6)

relatively low concentrations of protons and of the acid (3-MTPA) served to avoid competitive production of the intermolecularly S∴S-bonded dimeric radical cations **3a** through the water-assisted reaction[15] of the hydroxysulfuranyl radical (⟩$^\bullet$S−OH) with nonoxidized 3-MTPA (reaction 7) or through

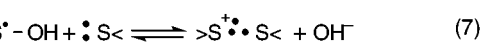

(7)

proton-catalyzed formation of monomeric sulfur radical cations (reaction 8) followed by association with a nonoxidized thioether

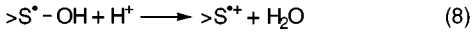

(8)

(reaction 9).

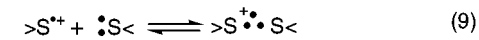

(9)

Under these experimental conditions, the radiation chemical yield of the hydroxyl radicals, available for reaction with 3-MTPA, was $G(^\bullet OH) = 5.3$ (based on the formula given by Schuler *et al.*[31] which relates the *G*-value of solute radicals generated by $^\bullet$OH to the product of the rate constant for the reaction of $^\bullet$OH with the solute and the solute concentration). Assuming the yield of intramolecularly sulfur−oxygen bonded radicals to be equal to the initial yield of the hydroxysulfuranyl radicals, ⟩$^\bullet$S−OH (where these yields are equal to 80% of the total available $^\bullet$OH radicals),[8a,18c] we derive $G(^\bullet S{\leftrightarrow}O) \approx 4.25$ and the molar aborption coefficient $\epsilon_{390} = 2500$ M^{-1} cm^{-1} for **2a** which compares well with values of $\epsilon_{390-400} = 2000-4000$ M^{-1} cm^{-1} for other ($^\bullet S{\leftrightarrow}O$)-bonded radicals.[18a,32] For a better comparison, all extinction coefficients derived for the various intermediates are summarized in Table 1.

Intermolecularly S∴S-bonded dimeric radical cations **3a** were independently generated in N_2-saturated solutions containing a high concentration, 10^{-2} M, of 3-MTPA at pH 1. At such low pH, proton-assisted elimination of water from the initially formed hydroxysulfuranyl radical directly leads to dimeric sulfur-centered radical cations **3a** via reactions 8 and 9 (vide supra). On the basis of 80%[8a,18c] of the available $^\bullet$OH radicals (at pH 1.0, $G_{total} = 3.0$) converting into **3a**, we derive $G(S\therefore S)^+ = 2.4$ and the molar extinction coefficient $\epsilon_{480} = 9200$ M^{-1} cm^{-1} for **3a**. It compares well with $\epsilon_{480-500} = 4000-9000$ M^{-1} cm^{-1} for other $(R_2S\therefore SR_2)^+$ radical cations.[8a,12a,18bc,32−34]

TABLE 2: Radiation Chemical Yields (*G*) of $(S\therefore S)^+$- and ($S^\bullet$-O)-Bonded Radicals in the $^\bullet$OH-Induced Oxidation of 3-MTPA in N_2O-Saturated Solutions at pH 6

concentration (M)	$G(S\therefore S)^+$ [a]	$G(S^\bullet{-}O)$[a]
2.0×10^{-3}	0.6[b]	4.05[b]
1.0×10^{-2}	1.6[c]	3.3[c]
1.4×10^{-2}	1.65[c]	3.25[c]
2.9×10^{-2}	2.15[c]	2.75[c]
5.6×10^{-2}	2.45[c]	2.45[c]
1.0×10^{-1}	2.8[c]	2.1[c]

[a] Based on spectral mix (see text). [b] Calculated value taking $G(^\bullet OH)$ = 4.7 (80% of the available $^\bullet$OH radicals) as the sum of $G(S\therefore S)^+$ and $G(S^\bullet{-}O)$. [c] Calculated value taking $G(^\bullet OH) = 4.9$ (80% of the available $^\bullet$OH radicals) as the sum of $G(S\therefore S)^+$ and $G(S^\bullet{-}O)$.

The spectra of these radicals were then used as potential components in the analysis of the transient spectra following the $^\bullet$OH-induced oxidation. Figure 1B shows the spectral resolution of the transient absorption taken 50 ns after the pulse (Figure 1A, curve a). Two intermediates could be identified from the composite spectrum. The transient at 390 nm represents the intramolecularly ($^\bullet S{\leftrightarrow}O$)-bonded radical **2a** and that at 480 nm is assigned to the intermolecularly S∴S-bonded dimeric radical cation **3a**. As shown in Figure 1B, the presence of an intermediate absorbing in the short-wavelength region around 340 nm is required to get a reasonably good composite fit with the experimental data. On the basis of previous results,[13−16] this intermediate is suggested to be the hydroxysulfuranyl radical (⟩$^\bullet$S−OH) **1a** which, at 50 ns after the pulse has not been fully transformed either into species **2a** or **3a**. In contrast, Figure 1C shows the spectral resolution of the same system at 800 ns after the pulse (Figure 1A, curve b). There, the composite transient spectrum can be cleanly resolved into a contribution from **3a** along with a contribution from the **2a**. As at this time **1a** is completely converted either into **2a** or **3a**, no extra individual spectrum was needed to fit the transient spectrum.

Table 2 shows that the relative values of **2a** and **3a** were sensitive to the concentration of 3-MTPA with increasing ratios [**2a**]:[**3a**] with decreasing concentration of 3-MTPA. For example, for 2×10^{-3} M of 3-MTPA, keeping otherwise similar experimental conditions, the spectrum recorded at 190 ns after the pulse consists of an intense band with $\lambda_{max} = 390-400$ nm and a shoulder around 480 nm. That shoulder became more pronounced at 2 μs after the pulse. By resolving this (Figure 2, open circles) and other experimental transient absorption spectra, the two intermediates **2a** and **3a** were quantified for $(0.1-1.0) \times 10^{-1}$ M 3-MTPA (Table 2).

3,3′-Thiodipropionic Acid (3,3′-TDPA). Pulse radiolysis of N_2O- and N_2-saturated solutions of 3,3′-TDPA over the concentration range $2 \times 10^{-4}-10^{-1}$ M and the pH range 1−6 yielded similar transient species as compared with the solutions of 3-MTPA, i.e., intramolecularly ($^\bullet S{\leftrightarrow}O$)-bonded radicals **2b** and intermolecularly S∴S-bonded dimeric radical cations **3b** (see the respective structures in Chart 2). Despite this similarity, a remarkable difference between these two acids existed with respect to the ratios of *G* values of species **2b** and **3b** when these ratios were measured at the same pH and the same solute concentration.

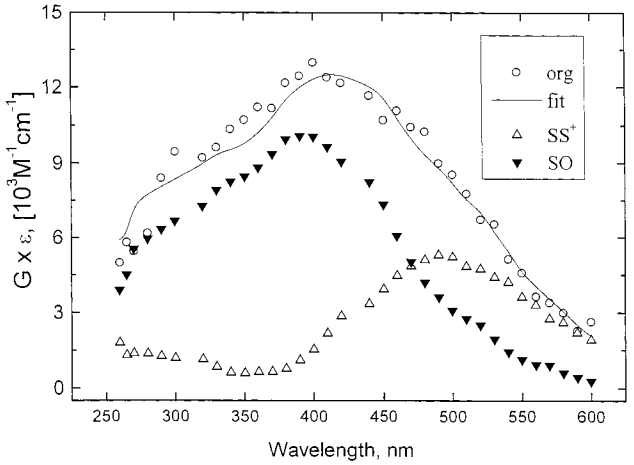

Figure 2. Resolution of the spectral components in the transient absorption spectrum following the •OH-induced oxidation of 3-MTPA (2×10^{-3} M) at pH 5.7 taken 2 μs after the pulse.

Pulse irradiation of an N_2O-saturated solution, pH 5.8, of $2 \times 10^{-3}-10^{-2}$ M of 3,3′-TDPA led to the formation of an absorption band with $\lambda_{max} = 400$ nm. Similar resolutions of the composite spectra (as performed for 3-MTPA solutions, vide supra) recorded 50 ns after the pulse for 10^{-2} M and 1.5 μs after the pulse for 2×10^{-3} M solution of 3,3′-TDPA showed that the spectra were primarily due to the intramolecularly (•S↔O)-bonded radicals **2b** with only a minor contribution of intermolecularly S∴S-bonded dimeric radical cations **3b** ($G < 0.05$) for 10^{-2} M solutions. After 30 μs, the transient absorption spectrum recorded in 10^{-2} M solution was still dominated by the 400 nm absorption, however, with a slightly higher contribution in it of the species **3b** with $G \approx 0.35$. At present, it is concluded that only a small part of the species **2b** might be converted into the species **3b**.

The spectrum of **2b** was independently obtained by pulse irradiation of an N_2O-saturated aqueous solution of 2×10^{-4} M of 3,3′-TDPA at pH = 6.0 yielding the molar extinction coefficient $\epsilon_{390} = 2900$ M^{-1} cm^{-1}.

An additional interesting feature was observed in N_2-saturated solutions of 3,3′-TDPA, at pH 1. As shown in Figure 3A, (solid circles), the transient spectrum recorded 230 ns after pulse irradiation of a 10^{-2} M solution of 3,3′-TDPA was reminiscent of **3b**. Division of $G\epsilon_{500} = 14\,800$ M^{-1} cm^{-1} by $G = 2.4$ yielded an apparent $\epsilon_{500} = 6200$ M^{-1} cm^{-1}, i.e., a molar extinction coefficient that is more than 30% lower than the value of ϵ_{480} for **3a**, (vide supra). This supports the conjecture of the presence of an additional species, very likely of **2b**, even at such high 3,3′-TDPA concentration at pH 1. In order to obtain ϵ_{500} through an exclusive formation of **3b**, experiments were carried out in 10^{-1} M solution of 3,3′-TDPA. Division of $G\epsilon_{500} = 19800$ M^{-1} cm^{-1} by $G = 2.4$ then yields $\epsilon_{500} = 8250$ M^{-1} cm^{-1} for **3b**, which is comparable to the value of $\epsilon_{480} = 9200$ M^{-1} cm^{-1} for **3a**.

As for 3-MTPA, the relative yields of **2b** and **3b** were sensitive to the concentration of 3,3′-TDPA. Representative experimental spectra for 2×10^{-3} M solution of 3,3′-TDPA recorded 80 ns (Figure 3B, curve a) and 1.5 μs (Figure 3B, curve b) after the pulse consisted only of broad, flat absorption bands in the range of 350−470 nm. Resolutions of the spectra (Figure 3, C and D) showed a superposition of the absorption band of **2b** with $\lambda_{max} = 390$ nm and **3b** with $\lambda_{max} = 500$ nm. The respective G-values of **2b** and **3b** for ($10^{-2}-10^{-1}$ M) solutions of 3,3′-TDPA at pH 6 and 2×10^{-3} and 10^{-2} M solutions of 3,3′-TDPA at pH 1 are shown in Table 3.

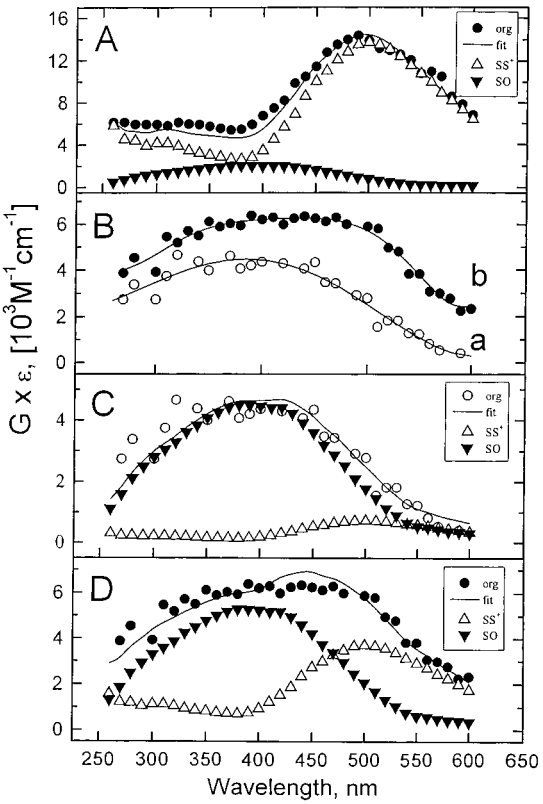

Figure 3. (A) Resolution of the spectral components in the transient absorption spectrum following the •OH-induced oxidation of 3,3′-TDPA (10^{-2} M) at pH 1.0 taken 230 ns after the pulse. (B) Transient absorption spectra observed (a) 80 ns and (b) 1.5 μs after pulse irradiation of an N_2-saturated aqueous solution containing 2×10^{-3} M 3,3′-TDPA at pH 1.0. (C) Resolution of the spectral components in the transient absorption spectrum following the •OH-induced oxidation of 3,3′-TDPA (2×10^{-3} M) at pH 1.0 taken 80 ns after the pulse. (D) Resolution of the spectral components in the transient absorption spectrum following the •OH-induced oxidation of 3,3′-TDPA (2×10^{-3} M) at pH 1.0 taken 1.5 μs after the pulse.

TABLE 3: Radiation Chemical Yields (G) of $(S\therefore S)^+$- and (S•−O)-Bonded Radicals in the •OH-Induced Oxidation of 3,3′-TDPA in N_2O-Saturated Solutions at pH 6 and 1

concentration (M)	$G(S\therefore S)^+$ [a]	G(S•−O)[a]
1.0×10^{-2} [b]	<0.05	4.85
2.1×10^{-2} [b]	0.15[c]	4.75[c]
4.2×10^{-2} [b]	0.4[c]	4.5[c]
6.5×10^{-2} [b]	0.65[c]	4.25[c]
1.0×10^{-1} [b]	1.0[c]	3.9[c]
2.0×10^{-3} [d]	0.4[e]	1.8[e]
1.0×10^{-2} [d]	1.7[f]	0.7[f]

[a] Based on spectral mix (see text). [b] pH = 6.0, N_2O-saturated. [c] Calculated value taking G(•OH) = 4.9 (80% of the available •OH radicals) as the sum of $G(S\therefore S)^+$ and G(•S−O). [d] pH = 1.0, N_2-saturated. [e] Calculated value taking G(•OH) = 2.2 (80% of the available •OH radicals) as the sum of $G(S\therefore S)^+$ and G(•S−O). [f] Calculated value taking G(•OH) = 2.4 (80% of the available •OH radicals) as the sum of $G(S\therefore S)^+$ and G(•S−O).

3-(Carboxymethylthio)propionic Acid (3-CMTPA). With respect to the sulfur, 3-CMTPA contains α- and β-positioned carboxylate groups. The transient absorption spectrum recorded in a pulse irradiated N_2O-saturated solution of 3-CMTPA (10^{-2} M) at pH 5.8, 20 ns after the pulse (Figure 4A, curve a), consisted of at least two absorption bands in the UV, one with a maximum around 340 nm and a second with a maximum around 290 nm. Subsequently, the absorption at 340 nm converted into a spectrum with $\lambda_{max} = 285$ nm (Figure 4A, curve

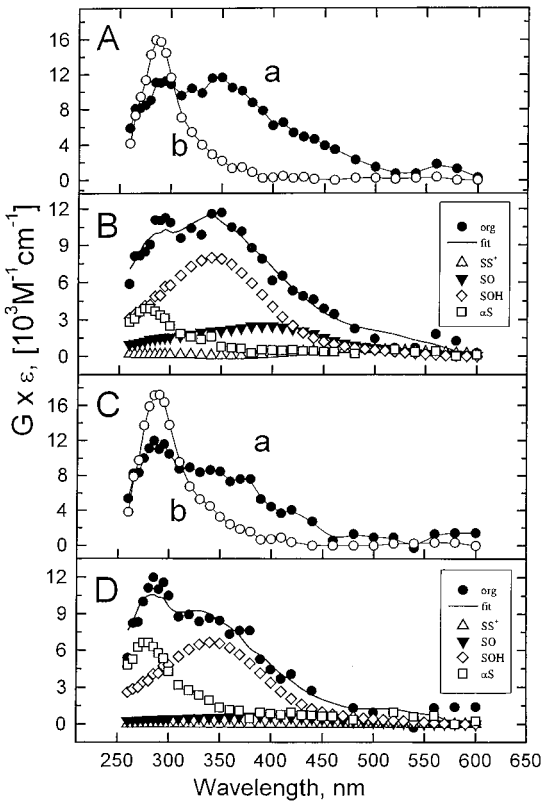

Figure 4. (A) Transient absorption spectra observed (a) 20 ns and (b) 745 ns after pulse irradiation of an N_2O-saturated aqueous solution containing 10^{-2} M 3-CMTPA at pH 5.8. (B) Resolution of the spectral components in the transient absorption spectrum following the •OH-induced oxidation of 3-CMTPA (10^{-2} M) at pH 5.8 taken 20 ns after the pulse. (C) Transient absorption spectra observed (a) 40 ns and (b) 1.5 μs after pulse irradiation of an N_2O-saturated aqueous solution containing 10^{-2} M 2-CMTSA at pH 5.8. (D) Resolution of the spectral components in the transient absorption spectrum following the •OH-induced oxidation of 2-CMTSA (10^{-2} M) at pH 5.8 taken 40 ns after the pulse.

b), with $k = 2.7 \times 10^7$ s^{-1}. By analogy with similar findings for α-carboxyalkyl sulfides,[16] the absorption band with $\lambda_{max} =$ 340 nm represents a hydroxysulfuranyl radical (⟩S•−OH) **1c** which rapidly converts via decarboxylation into an α-(alkylthio)-alkyl radical •CH_2SCH_2R (R = H, COOH) (known to absorb in the 280−310 nm region with extinction coefficients of 2000−3000 M^{-1} cm^{-1})[9c,15,16] (Figure 4A, curve b). In competition to direct decarboxylation, the hydroxysulfuranyl radical can transform into the intramolecularly (S•↔O)-bonded species **2c** involving the β-carboxylate group, promoted by a sterically and kinetically favorable five-membered ring configuration. Evidence for this reaction pathway was obtained using the spectral resolution (vide supra) of the composite transient absorption spectrum taken 20 ns after the pulse (Figure 4A, curve a). As shown in Figure 4B, the composite transient spectrum can be resolved into a contribution from the hydroxysulfuranyl radical (⟩S•−OH) **1c**, the α-(alkylthio)alkyl radical (•$CH_2SCH_2CH_2$-COOH), but additionally shows the presence of the intramolecularly (S•↔O)-bonded radical **2c**.

The transient absorption spectra observed 50 ns and 1.5 μs after pulse irradiation of an N_2-saturated solution of 10^{-2} M 3-CMTPA at pH 1 consisted only of an intense absorption band with $\lambda_{max} = 285$ nm. Since no absorption in the region 370−600 nm was observed, it can be inferred that **2c** and **3c** were not formed.

2-(Carboxymethylthio)succinic Acid (2-CMTSA). 2-CMTSA contains three carboxylate groups, two in α- and one in β-position to the sulfur. The absorption spectra observed in solutions of 10^{-2} M 2-CMTSA at pH 5.8 and pH 1 were similar to those observed for 3-CMTPA. Here, the presence of two α-positioned carboxylate groups promoted a more efficient decarboxylation process as compared to 3-CMTPA. Hence the composite absorption spectrum recorded in a solution of 10^{-2} M 2-CMTSA at pH 5.8, 40 ns after the pulse (Figure 4C) contained a much smaller contribution of the intramolecularly (S•↔O)-bonded radical **2d** as compared to that of 3-CMTPA (vide supra), together with a contribution from the hydroxysulfuranyl radical (⟩S•−OH) **1d**, and the α-(alkylthio)alkyl radical (•$CH_2SCH(COO^-)CH_2COOH$) (Figure 4D).

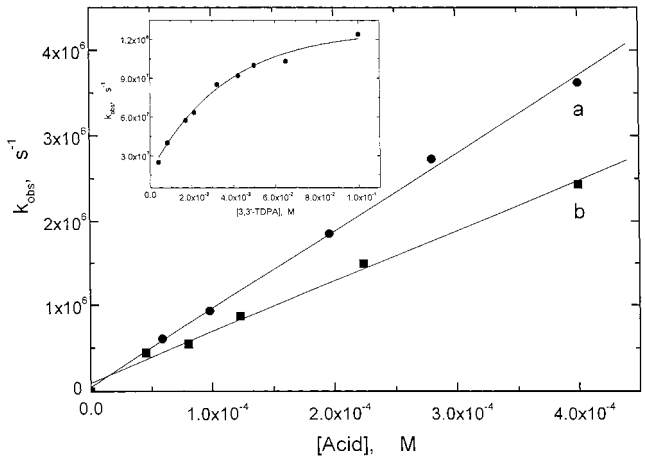

Figure 5. Plot of observed first-order rate constants of the formation of intramolecularly (•S−O)-bonded radicals (monitored at 400 nm) in N_2O-saturated aqueous solution at pH 5.8 as a function of 3-MTPA concentration (curve a) and as a function 3,3′-TDPA concentration (curve b) (low concentration region). Insert: Plot of observed first-order rate constants of the formation of an intramolecularly (•S−O)-bonded radical (monitored at 400 nm) at pH 5.8 in N_2O-saturated aqueous solution as a function of 3,3′-TDPA concentration (high concentration region).

Kinetics. *3-(Methylthio)propionic Acid (3-MTPA).* Since the decay of the initially formed hydroxysulfuranyl radical of 3-MTPA (**1a**) was very fast, the formation rate constant, $k_{OH+3\text{-MTPA}}$, was obtained from the experimentally measured pseudo-first-order rate constant, k_{obs}, for the formation of the intramolecularly (•S↔O)-bonded radicals **2a** at $\lambda = 400$ nm, under conditions where k_{10}[3-MTPA] ≪ k_{11}, i.e., for 3-MTPA concentrations between 5.9×10^{-5} and 4.0×10^{-4} M (pH 5.8).

$$\text{•OH} + \text{3-MTPA} \rightarrow \underset{\textbf{1a}}{\text{3-MTPA(⟩S•−OH)}} \qquad (10)$$

$$\underset{\textbf{1a}}{\text{3-MTPA(⟩S•−OH)}} \rightarrow \underset{\textbf{2a}}{\text{3-MTPA(•S↔O)}} + \text{OH}^- \qquad (11)$$

The rate constant, $k_{10} = k_{OH+3\text{-MTPA}} = (9.2 \pm 0.2) \times 10^9$ M^{-1} s^{-1}, was obtained by employing relation II:

$$k_{obs} = k_{10}[\text{3-MTPA}] \qquad \text{(II)}$$

A plot based on eq II is presented in Figure 5 (curve a).

The rate constant for the formation of **3a** (reaction 12) was obtained at high (>10^{-2} M) concentrations of substrate (3-MTPA). A typical experimental trace observed for monitoring the formation of **3a** at $\lambda = 480$ nm is presented in the insert of Figure 6. The formation was of pseudo-first-order kinetics with the rate constant, k'_{obs}, being linearly dependent on the 3-MTPA concentration. Figure 6 (curve a) shows a representative plot

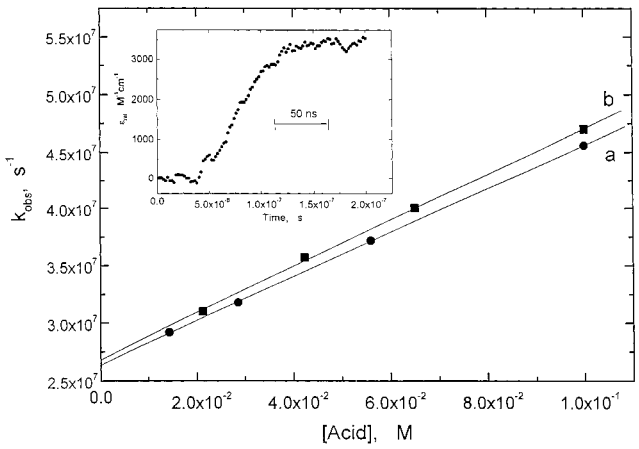

Figure 6. Plot of observed first-order rate constants of the formation of intermolecularly (S∴S)-bonded radicals (monitored at 480 nm for 3-MTPA and at 510 nm for 3,3′-TDPA) in N_2O-saturated aqueous solution at pH 5.8 at as a function of 3-MTPA concentration (curve a) and as a function 3,3′-TDPA concentration (curve b). Insert: Kinetic trace for the formation of intermolecularly (S∴S)-bonded radicals monitored at 480 nm (pulse radiolysis of N_2O-saturated aqueous solution of 1.4×10^{-2} M 3-MTPA at pH = 5.8).

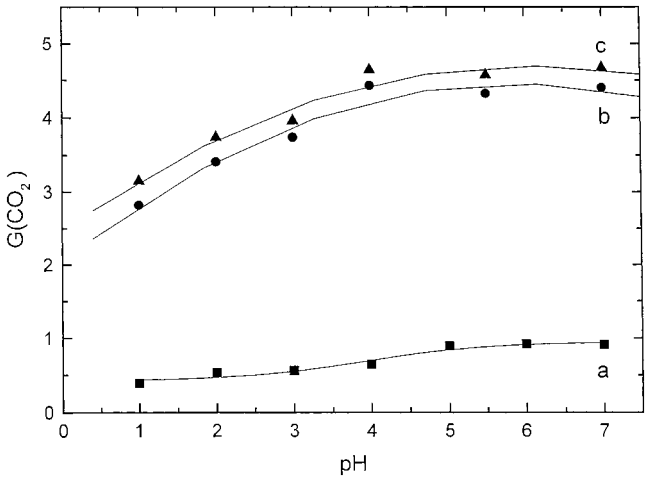

Figure 7. Radiation chemical yields (G values) of carbon dioxide (CO_2) obtained after γ-irradiation of N_2O-saturated aqueous solutions at various pH's containing 10^{-2} M (a) 3,3′-TDPA, (b) 3-CMTPA), and (c) 2-CMTSA).

of k'_{obs} vs various concentrations of 3-MTPA ($10^{-2}-10^{-1}$ M). The slope of this plot gives the bimolecular rate constant, $k_{12} = 1.9 \times 10^8$ M^{-1} s^{-1} for the reaction of a precursor of **3a**, here referred to as 3-MTPA($X^{\bullet}$), with a second nonoxidized 3-MTPA molecule (reaction 12).

$$\text{3-MTPA}(X^{\bullet}) + \text{3-MTPA} \rightarrow \underset{\mathbf{3a}}{\text{3-MTPA}(\rangle S \therefore S\langle)^+} + OH^- \quad (12)$$

At this moment, we will not attempt to specify the identity of this precursor (see Discussion). However, the fact that this plot intercepts the y-axis at 2.6×10^7 s^{-1} indicates that the precursor for the formation of **3a** can react via a competitive pathway.

3,3′-Thiodipropionic Acid (3,3′-TDPA). A similar set of experiments performed at low concentrations of 3,3′-TDPA ($4.6 \times 10^{-5}-4.0 \times 10^{-4}$ M) at pH 5.8 yielded $k_{OH+3,3'\text{-TDPA}} = k_{13} = (6.0 \pm 0.2) \times 10^9$ M^{-1} s^{-1}.

$$^{\bullet}OH + \text{3,3′-TDPA} \rightarrow \underset{\mathbf{1b}}{\text{3,3′-TDPA}(\rangle S^{\bullet}-OH)} \quad (13)$$

$$\underset{\mathbf{1b}}{\text{3,3′-TDPA}(\rangle S^{\bullet}-OH)} \rightarrow \underset{\mathbf{2b}}{\text{3,3′-TDPA}(^{\bullet}S\leftrightarrow O)} + OH^- \quad (14)$$

The rate constant k_{13} was obtained from the plot of experimentally measured pseudo-first-order rate constants, k''_{obs}, for the formation of **2b** at $\lambda = 400$ nm (Figure 5, curve b) at various concentrations of 3,3′-TDPA by employing the same type of relation (see eq II) as for 3-MTPA. At high 3,3′-TDPA concentrations, however, the plot of k''_{obs} vs [3,3′-TDPA] showed a departure from linearity (Figure 5, insert), and at [3,3′-TDPA] > 4×10^{-2} M, k''_{obs} approached a constant value of ca. 1.2×10^8 s^{-1}. Such kinetic behavior is indicative of a two-step mechanism for the formation of the ($^{\bullet}S\leftrightarrow O$)-bonded radical (reactions 13 and 14), with reaction 14 becoming rate determining at high concentrations of 3,3′-TDPA. The respective plateau value refers to the first-order rate constant, k_{14}, for the decay of the hydroxysulfuranyl radical by a carboxylate-assisted elimination of OH^- and formation of the intramolecularly ($^{\bullet}S\leftrightarrow O$)-bonded radical.

For 3,3′-TDPA, the yields of the ($^{\bullet}S\leftrightarrow O$)-bonded radical **2b** at pH 5.8 were high even at high concentrations of the solute (see Table 3) due to the presence of two β-carboxyethyl substituents at the sulfur which can form kinetically favorable five-membered rings. As in the case of 3-MTPA, when the concentration of 3,3′-TDPA was high enough ($> 2 \times 10^{-2}$ M), the experimental traces clearly indicated the formation of the intermolecularly S∴S-bonded dimeric radical cations **3b** from 3,3′-TDPA ($\lambda_{max} = 500$ nm). Using an analogous procedure as for 3-MTPA, a similar plot of k'''_{obs} for various concentrations of 3,3′-TDPA ($2 \times 10^{-2}-10^{-1}$ M) was obtained (Figure 6, curve b). The slope of this plot gives the bimolecular rate constant, $k_{15} = 2.0 \times 10^8$ M^{-1} s^{-1}, for the reaction of the precursor(s) of **3b** formed during $^{\bullet}OH$-induced oxidation of 3,3′-TDPA with the second nonoxidized 3,3′-TDPA molecule (reaction 15).

$$\text{3,3′-TDPA}(X^{\bullet}) + \text{3-TDPA} \rightarrow \underset{\mathbf{3b}}{\text{3,3′-TDPA}(\rangle S \therefore S\langle)^+} + OH^- \quad (15)$$

The intercept of this plot (Figure 6, curve b) yields the combined rate constant, $k_{incpt} = 2.7 \times 10^7$ s^{-1}, for the decay of precursor(s) of **3** via processes other than reaction 15. Importantly, this intercept is too low in order to contain $k_{14} = 1.2 \times 10^8$ M^{-1} s^{-1}, indicating that **1b** cannot be a direct precursor of **3b**.

γ-Radiolysis. Decarboxylation. The γ-irradiation of N_2O-saturated solutions of 10^{-2} M 3,3′-TDPA, 3-CMTPA, and 2-CMTSA in the pH range 1.0−7.0 resulted in the formation of CO_2 (Figure 7). For better assessment of decarboxylation yields, the $G(CO_2)$ values were normalized to the total initial radiation chemical yield of $^{\bullet}OH$ radicals at the particular pH. The respective data are summarized in Table 4. For 3,3′-TDPA at pH 1−4 the efficiency of CO_2 formation corresponded to about 11% of the total yields of $^{\bullet}OH$ radicals. A slightly higher efficiency of CO_2 formation (∼15% of the total yield of $^{\bullet}OH$ radicals) was obtained at pH 5−7. Considerably higher yields of CO_2 were quantified after γ-irradiation of N_2O-saturated solutions containing 3-CMTPA and 2-CMTSA (at pH 1 85% and 95% and at pH 5−7 ∼72% and ∼76% of the total yield of $^{\bullet}OH$ radicals, respectively).

Discussion

Key Features of the $^{\bullet}OH$-Induced Oxidation of (Carboxyalkyl)thiopropionic Acid Derivatives. There are several key

TABLE 4: Radiation Chemical Yields of the •OH-Induced CO_2 Formation (in G) and Efficiency of Decarboxylation (Expressed as $f = G(CO_2)_{exp}/G(•OH)_{pH}$[a]) in N_2O-Saturated Solutions of (Carboxyalkyl)thiopropionic Acids (10^{-2} M)

	3,3′-TDPA		3-CMTPA		2-CMTSA	
pH	G[b,c]	f	G[b,c]	f	G[b,c]	f
1	0.39	0.12	2.82	0.85	3.15	0.95
2	0.53	0.12	3.41	0.77	3.74	0.84
3	0.56	0.10	3.74	0.65	3.96	0.69
4	0.64	0.11	4.43	0.73	4.64	0.77
5	0.89	0.15				
5.5			4.32	0.71	4.57	0.75
6	0.92	0.15				
7	0.91	0.15	4.40	0.72	4.67	0.77

[a] The total initial radiation chemical yield of •OH radicals at particular pH was calculated according to the formula: $[G(•OH) + G(e_{aq}^-)]/k_{e+N_2O}[N_2O]/k_{e+N_2O}[N_2O] + k_{e+H+}[H^+]$. [b] Measured by the GC technique (pH = 1−3). [c] Measured by the HPIC technique (pH = 4−7).

features that are important to consider for a discussion of the mechanism of the •OH-induced oxidation of (carboxyalkyl)-thiopropionic acid derivatives. (i) The oxidation leads to the intramolecularly (•S↔O)-bonded radicals **2a**−**d** predominantly at low concentrations of substrate and protons. (ii) In the absence of carboxylate groups in α-position to the sulfur, the formation of intermolecularly S∴S-bonded dimeric radical cations **3a/b** is promoted by high concentrations of substrate and protons, and by an overall decreasing number of carboxylate groups. (iii) At low proton concentrations ($\leq 10^{-6}$ M) the first-order rate constant for a transformation of hydroxysulfuranyl radicals into intramolecularly (•S↔O)-bonded radicals (**2b** for 3,3′-TDPA) is very high ($k_{14} \cong 10^8$ s^{-1}) whereas the first- or pseudo-first-order rate constants for a decay of precursor(s) of **3a/b** via processes other than reaction 12 (for 3-MTPA) or 15 (for 3,3′-TDPA) are in the range of $(2.6-2.7) \times 10^7$ s^{-1}. (iv) The bimolecular rate constants for the formation of **3a/b** (reaction 12 for 3-MTPA or 15 for 3,3′-TDPA) are in the range of $(1.9-2.0) \times 10^8$ M^{-1} s^{-1}. (v) The oxidation results in CO_2 with low yields for 3,3′-TDPA and high yields for 3-CMTPA and 2-CMTSA at pH 1−7.

Possible Reactions and Intermediates. The first step in the reaction of hydroxyl radicals with thioethers is generally an addition to the sulfur leading to the hydroxysulfuranyl-type radicals (reactions 10 and 13) which are characterized by an optical absorption band in the 330−340-nm range.[13,15,16,35] The subsequent reactions of these species then depend on pH, solute concentration, and the presence of additional functionalities. For 3-MTPA and 3,3′-TDPA, these mechanisms are shown in reactions 10, 11/13, 14, and 16−19. At low proton concentration, decomposition of the hydroxysulfuranyl radical can occur via the following pathways. (i) A unimolecular dissociation generates the monomeric sulfur-centered radical cation (reaction 16)

$$\underset{\textbf{1a/b}}{\text{3-MTPA/3,3′-TDPA}(\rangle S^{\bullet}-OH)} \rightarrow \text{3-MTPA/3,3′-TDPA}(\rangle S^{\bullet+}) + OH^- \quad (16)$$

which subsequently either associates with a second thioether molecule (reaction 17) or cyclizes to the intramolecularly (•S↔O)-bonded radicals **2a/b** (reaction 18).

$$\text{3-MTPA/3,3′-TDPA}(\rangle S^{+\bullet}) + \text{3-MTPA/3,3′-TDPA} \rightarrow \underset{\textbf{3a/b}}{\text{3-MTPA/3,3′-TDPA}(\rangle S\therefore S\langle)^+} \quad (17)$$

$$\text{3-MTPA/3,3′-TDPA}(\rangle S^{+\bullet}) \rightarrow \underset{\textbf{2a/b}}{\text{3-MTPA/3,3′-TDPA}(^{\bullet}S\leftrightarrow O)} \quad (18)$$

(ii) A displacement of OH^- by a second thioether molecule directly leads to **3a/b** (reaction 19).

$$\underset{\textbf{1a/b}}{\text{3-MTPA/3,3′-TDPA}(\rangle S^{\bullet}-OH)} + \text{3-MTPA/3,3′-TDPA} \rightarrow \underset{\textbf{3a/b}}{\text{3-MTPA/3,3′-TDPA}(\rangle S\therefore S\langle)^+} + OH^- \quad (19)$$

(iii) Intramolecular displacement of OH^- by the neighboring carboxylate group(s) leads to the intramolecularly (•S↔O)-bonded radicals **2a/b** (reactions 11 and 14).

Under our experimental conditions, the unimolecular dissociation of the hydroxy-sulfuranyl radical (reaction 16) can likely be disregarded as a competitive process at neutral pH, as such reactions typically proceed with rate constants on the order of 10^4-10^6 s^{-1}, [8a,13,16,36] i.e., too slow to account for the observed conversion of **1b** into **2b** with $k_{14} = 1.2 \times 10^8$ s^{-1}. Thus, at neutral pH, one potential mechanism leading to **2a/b** is the direct displacement of OH^- by the carboxylate groups (reactions 11 and 14). However, our kinetic analysis below will demonstrate an additional pathway for the formation of **2a/b**.

Ultimately, hydroxysulfuranyl radicals can yield **3a/b**. If reactions 11/14 and 19 were the only two competitive processes the G value of **3a/b** would be related to the concentration of substrate (3-MTPA or 3,3′-TDPA) according to eq III where $G^0(3)$ is the primary yield of the precursor (⟩S•−OH), and $G(3)$ is the actual yield of **3a/b** (taken from Tables 2 and 3).

$$\frac{G^0(3)}{G(3)} = 1 + \frac{k_{11,14}}{k_{19}} \times \frac{1}{[\text{substrate}]} \quad \text{(III)}$$

However, plots of $(G^0(3)/G(3))$ vs 1/[substrate] (Figure 8) show a significant departure from linearity indicating a more complex reaction mechanism. This, in turn, eliminates hydroxysulfuranyl radicals **1a/b** as direct precursors of the intermolecularly S∴S-bonded dimeric radical cations **3a/b**. Further convincing evidence against the hydroxysulfuranyl radical as a direct precursor of **3a/b**, at least for 3,3′-TDPA, can be deduced from the value of the intercept obtained from the plot of k'''_{obs} at various concentrations of 3,3′-TDPA (see Figure 6, curve b). Since this value represents a first- or pseudo-first-order rate constant for a decay of precursor(s) of **3b** via processes other than reaction 15, it should contain also k_{14} ($\sim 1.2 \times 10^8$ s^{-1}); however, the measured value is 4-fold lower (2.7×10^7 s^{-1}). This excludes any significant contribution of reaction 19 to the formation of **3b**.

Mechanism. The following mechanism accounts for all experimental results and particularly for the fact that reactions 11/14 and 19 are not the exclusive competitive processes that lead to formation of the intramolecularly (•S↔O)-bonded radicals **2a/b** and the intermolecularly S∴S-bonded dimeric radical cations **3a/b**, respectively. Depending on the actual pH, solute concentration, and the number of carboxylate groups, the initially formed hydroxysulfuranyl radicals **1a/1b** undergo a proton-catalyzed elimination (reaction 8) and/or the displacement of hydroxide ions by a second thioether molecule (reaction 19). An additional reaction channel provides the basis for the observation of the intramolecularly (•S↔O)-bonded radicals **2b** of 3,3′-TDPA even at low pH and high solute concentration (see Table 3). We propose that the hydroxysulfuranyl radical **1b** undergoes a rapid cyclization (Scheme 1, reaction 1.1) to

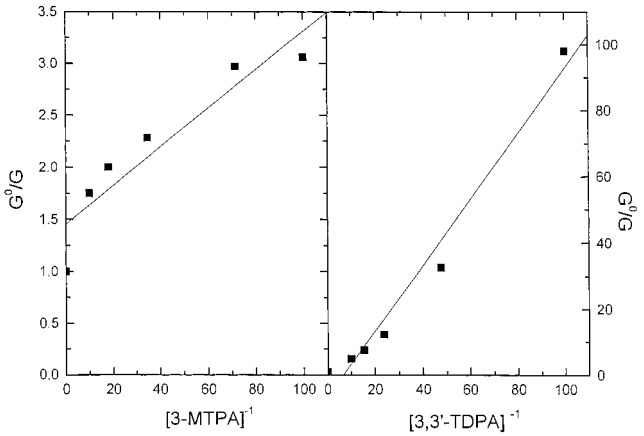

Figure 8. Plots of G^0/G vs 1/[3-MTPA] (left) and 1/[3,3′-TDPA] (right) according to eq III. The straight lines were obtained by linear regression and are displayed only to demonstrate the departure of the data from linearity.

SCHEME 1

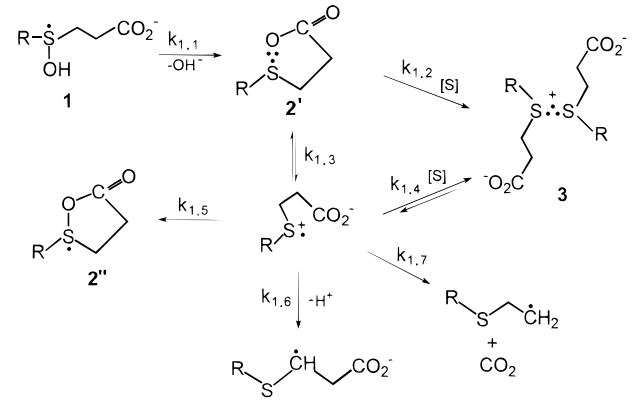

the σ^*-type intramolecularly (S∴O)-bonded radicals **2′b** characterized by a two-center-three-electron bond between the sulfur and the oxygen (consistent with an optical absorption band in the 390-nm range).[17,18] Subsequently, **2′b** undergoes either of two reactions: (i) displacement of the carboxylate group through the attack of a second unoxidized thioether molecule, directly leading to **3b** (Scheme 1, reaction 1.2) and (ii) reversible opening of the S∴O bond to the monomeric sulfur-centered radical cation (Scheme 1, reaction 1.3). The latter can reversibly associate with a second thioether molecule (Scheme 1, reaction 1.4). However, the fact that the plot of G^0/G vs 1/[substrate] is not linear (Figure 8) suggests that the monomeric sulfur-centered radical cation reacts via an additional channel. We propose that this additional channel represents an irreversible cyclization to the σ-type (instead of the σ^*-type) intramolecularly (•S−O)-bonded sulfuranyl radical **2″b** (Scheme 1, reaction 1.5). The experimentally observed absorption with $\lambda_{max} = 390$ nm is consistent with such an assignment. An important detail supporting this experimental conclusion is that the sum of absorbances at both 390 and 500 nm remains constant over the time period of observation; i.e., the additional irreversible reaction channel cannot be deprotonation in α-position to the sulfur within the time window of the experiment. Thus, the occurrence of this second type of (S−O)-bonded species is necessary in order to rationalize the presence of a 390 nm absorption band together with the fact that both the (S∴S)- and the (S−O)-bonded species are not formed competitively. Though specifically recognizable for 3,3′-TDPA, such pathways should be possible also for all the other investigated (carboxylalkyl)-thiopropionic acids.

On a longer time scale, experiments carried out with 10^{-2} M of 3,3′-TDPA at pH 5.9 did not show any significant transformation of **2′b** into the dimeric sulfur radical cation **3b**. Species **2′b** is expected to be in equilibrium with the monomeric radical cation (via reaction 1.3) and should in principle undergo transformation into species **3b** (via reaction 1.4) if cyclization to the sulfuranyl-type radical **2″b** (via reaction 1.5) was not favorable. We note that at neutral pH the formation of **3b** requires the contact between a monoanion (net charge of the monomeric sulfur radical cation of 3,3′-TDPA is −1) and a dianion. Thus, Coulombic repulsion within **3b** may favor the ultimate formation of **2″b** (reaction 1.5). In contrast, there is no net repulsion in complex **3a**, eventually rationalizing the different kinetic characteristics (no saturation) of the conversion of **1a** into **2a** for 3-MTPA. Our earlier findings with 3,3′-dihydroxydipropyl sulfide (3,3′-DHP)[15] provide an additional example for the effective formation of intermolecularly sulfur−sulfur-bonded species in the absence of Coulombic repulsion. During the •OH-induced oxidation of 3,3′-DHP at neutral pH (≈7) and at high solute concentraton (10^{-2} M) the spectrum attributed to the intramolecularly (S∴O)-bonded species disappears in a first-order process with $\tau_{1/2} = 6.3$ μs paralleled by the buildup of the spectrum attributed to the three-electron-bonded dimeric thioether radical cation of 3,3′-DHP.

In principle, the monomeric sulfur-centered radical cations derived from thioether acids can undergo one of three irreversible processes: (i) deprotonation at the carbon in the α-position to the sulfur yielding α-(alkylthio)alkyl radicals (Scheme 1, reaction 1.6), (ii) formation of the σ-type intramolecularly (•S−O)-bonded sulfuranyl radical (Scheme 1, reaction 1.5), and (iii) intramolecular electron transfer from the carboxyl group to the oxidized sulfur function followed by homolytic carbon−carboxyl breakage into carbon dioxide and the α-(alkylthio)-alkyl radical (Scheme 1, reaction 1.7). Decarboxylation for both 3-CMTPA and 2-CMTSA constitutes the ultimate pathway reflected by the nearly stoichiometric ratio of CO_2 and hydroxyl radicals initially reacting via one-electron oxidation (ca. 80%). This latter finding supports the existence of an equilibrium between the σ^*-type intramolecularly (•S−O)-bonded sulfuranyl radicals and the monomeric sulfur radical cations (Scheme 1, reaction 1.3). In particular, for 3-CMTPA, the formation of **2′c** was experimentally detectable.

In conclusion, this paper demonstrates that different sulfur radical cation complexes such as the (S∴S)- and (S−O)-bonded species from (carboxyalkyl)thiopropionic acids are not necessarily formed competitively, rationalized by the fact that in particular the (S−O)-bonded intermediates can adopt several distinct electronic configurations. Even though the σ^*- and σ-type S−O bond cannot be distinguished UV spectroscopically, our kinetic evidence suggests that both intermediates are present after one-electron oxidation of the thiopropionic acid derivatives.

Acknowledgment. This work was supported by the Office of Basic Energy Sciences of the Department of Energy and, as such, it is contribution No. NDRL-4081 from the Notre Dame Radiation Laboratory, and by NIH PO1 AG12993.

References and Notes

(1) Vogt, W. *Free Radical Biol. Med.* **1995**, *18*, 93−105.
(2) Moreno, J.; Pryor, W. A. *Chem. Res. Toxicol.* **1992**, *5*, 425−431.
(3) Pryor, W. A.; Jin, X.; Squadrito, G. L. *Proc. Natl. Acad. Sci. U.S.A.* **1994**, *91*, 11173−11177.
(4) Pryor, W. A.; Squadrito, G. L. *Am. J. Physiol.* **1995**, *268*, L699-L725.
(5) Hühmer, A. F. R.; Gerber, N. C.; Ortiz de Montelano, P. R.; Schöneich, C. *Chem. Res. Toxicol.* **1996**, *9*, 484−491.

(6) Jensen, J. L.; Miller, B. L.; Zhang, X.; Hug, G. L.; Schöneich, C. *J. Am. Chem. Soc.* **1997**, *119*, 4749−4757.

(7) Asmus, K. D. In *Sulfur-Centered Reactive Intermediates in Chemistry and Biology;* Chatgilialoglu, C., Asmus, K.-D., Eds.; NATO ASI Series, Series A: Life Sciences; Plenum Press: New York, 1990; Vol. 197, pp 155−172.

(8) (a) Hiller, K.-O.; Masloch, B.; Göbl, M.; Asmus, K.-D. *J. Am. Chem. Soc.* **1981**, *103*, 2734−2743. (b) Hiller, K.-O.; Asmus, K.-D. *J. Phys. Chem.* **1983**, *87*, 3682−3688.

(9) (a) Bobrowski, K.; Schöneich, C.; Holcman, J.; Asmus, K.-D. *J. Chem. Soc., Perkin Trans. 2* **1991**, 353−362. (b) Bobrowski, K.; Schöneich, C.; Holcman, J.; Asmus, K.-D. *J. Chem. Soc., Perkin Trans. 2* **1991**, 975−980. (c) Schöneich, C.; Zhao, F.; Madden, K. P.; Bobrowski, K. *J. Am. Chem. Soc.* **1994**, *116*, 4641−4652. (d) Bobrowski, K.; Schöneich, C. *Radiat. Phys. Chem.* **1996**, *47*, 507−510.

(10) Glass, R. S. In *Sulfur-Centered Reactive Intermediates in Chemistry and Biology;* Chatgilialoglu, C., Asmus, K.-D., Eds.; NATO ASI Series, Series A: Life Sciences; Plenum Press: New York, 1990; Vol. 197, pp 213−226.

(11) Droee, A. T.; Tully, F. P. *J. Phys. Chem.* **1986**, *90*, 1949−1954.

(12) (a) Bonifačić, M.; Möckel, H.; Bahnemann, D.; Asmus, K.-D. *J. Chem. Soc., Perkin Trans. 2* **1975**, 675−685. (b) Janata, E.; Veltwisch, D.; Asmus, K.-D. *Radiat. Phys. Chem.* **1980**, *16*, 43−49. (c) Asmus, K.-D.; Bahnemann, D.; Fischer, Ch.-H.; Veltwisch, D. *J. Am. Chem. Soc.* **1979**, *101*, 5322−5329.

(13) Bobrowski, K.; Schöneich, C. *J. Chem. Soc., Chem. Commun.* **1993**, 795−797.

(14) Schöneich, C.; Bobrowski, K. *J. Phys. Chem.* **1994**, *98*, 12613−12620.

(15) Schöneich, C.; Bobrowski, K. *J. Am. Chem. Soc.* **1993**, *115*, 6538−6547.

(16) Bobrowski, K.; Pogocki, D.; Schöneich, C. *J. Phys. Chem.* **1993**, *97*, 13677−13684.

(17) (a) Chatgilialoglu, C.; Castelhano, A. L.; Griller, D. *J. Org. Chem.* **1985**, *50*, 2516−2518. (b) Chatgilialoglu, C. In *The Chemistry of Sulphenic Acids and their Derivatives;* Patai, S., Ed.; John Wiley & Sons Ltd.: New York, 1990; Chapter 12, pp 549−569. (c) Perkins, C.; Martin, J. C.; Arduengo, A. J.; Lau, W.; Alegria, A.; Kochi, J. K. *J. Am. Chem. Soc.*, **1980**, *102*, 7753−7759. (d) Giles, J. R. M.; Roberts, B. P. *J. Chem. Soc., Perkin Trans. 2* **1980**, 1497−1504. (e) Morton, J. R.; Preston K. F. *J. Phys. Chem.* **1973**, *77*, 2645−2651.

(18) (a) Steffen, L. K.; Glass, R. S.; Sabahi, M.; Wilson, G. S.; Schöneich, C.; Mahling, S.; Asmus, K.-D. *J. Am. Chem. Soc.* **1991**, *113*, 2141−2145. (b) Bobrowski, K.; Holcman, J. *J. Phys. Chem.* **1989**, *93*, 6381−6387. (c) Asmus, K.-D.; Göbl, M.; Hiller, K.-O.; Mahling, S.; Mönig, J. *J. Chem. Soc., Perkin Trans. 2* **1985**, 641−646. (d) Glass, R. S.; Hojjatie, M.; Wilson, G. S.; Mahling, S.; Göbl, M.; Asmus, K.-D. *J. Am. Chem. Soc.* **1984**, *106*, 5382−5383. (e) Mohan, H.; Mittal, J. P. *J. Chem. Soc., Perkin Trans. 2* **1992**, 207−212. (f) Mohan, H. *J. Chem. Soc., Perkin Trans. 2* **1990**, 1821−1824.

(19) Marciniak, B.; Bobrowski, K.; Hug, G. L.; Rozwadowski, J. *J. Phys. Chem.* **1994**, *98*, 4854−4860.

(20) Schuler, R. H.; Patterson, L. K.; Janata, E. *J. Phys. Chem.* **1980**, *84*, 2088−2090.

(21) Janata, E.; Schuler, R. H. *J. Phys. Chem.* **1982**, *86*, 2078−2084.

(22) Schuler, R. H. *Chem. Educ. (Ind. Ed.)* **1985**, *2*, 34−57.

(23) Wang, Y. Unpublished report, 1993.

(24) Fricke, H.; Hart, E. J. In *Radiation Dosimetry*; Attix, T. H., Roesch, W. C., Eds.; Academic Press: New York, 1966.

(25) Mönig, J.; Chapman, R.; Asmus, K.-D. *J. Phys. Chem.* **1985**, *89*, 3139−3144.

(26) von Sonntag, C. *The Chemical Basis of Radiation Biology*: Taylor & Francis: London, 1987.

(27) Buxton, G. V.; Greenstock, C. L.; Helman, W. P.; Ross, A. *J. Phys. Chem. Ref. Data* **1988**, *17*, 513−866.

(28) This nonspecific notation does not specify electron localization in the sulfur−oxygen bonded radicals.

(29) Bevington, P. R. In *Data Reduction and Error Analysis for the Physical Sciences*; McGraw-Hill: New York, 1969.

(30) Marciniak, B.; Bobrowski, K.; Hug, G. L. *J. Phys. Chem.* **1993**, *97*, 11937−11943.

(31) Schuler, R. H.; Hartzell, A. L.; Behar, B. *J. Phys. Chem.* **1981**, *85*, 192−199.

(32) Mahling, S.; Asmus, K.-D.; Glass, R. S.; Hojjatie, M.; Wilson, G. S. *J. Org. Chem.* **1987**, *52*, 3717−3724.

(33) Mohan, H.; Mittal, J. P. *Radiat. Phys. Chem.* **1991**, *38*, 45−50.

(34) Holcman, J.; Bobrowski, K., Schöneich, C., Asmus, K.-D. *Radiat. Phys. Chem.* **1991**, *37*, 473−478.

(35) Asmus, K.-D., Bahnemann, D., Bonifačić, M., Gillis, H. A. *Dicuss. Faraday Chem. Soc.* **1975**, *63*, 213−235.

(36) Mönig, J., Goslich, R., Asmus, K.-D. *Ber. Bunsen-Ges. Phys. Chem.* **1986**, *90*, 115−121.